Femtosecond two-photon-excited backward lasing of atomic hydrogen in a flame

Ding, Pengji; Ruchkina, Maria; Yi, L. I.U.; Alden, Marcus; Bood, Joakim

Published in:
Optics Letters

DOI:
10.1364/OL.43.001183

2018

Document Version:
Publisher's PDF, also known as Version of record

Optics Letters

Femtosecond two-photon-excited backward lasing of atomic hydrogen in a flame

Pengji Ding,[1,*] Maria Ruchkina,[1] Yi Liu,[2] Marcus Alden,[1] and Joakim Bood[1]

[1]Department of Physics, Lund University, SE-22100 Lund, Sweden
[2]Shanghai Key Lab of Modern Optical System, University of Shanghai for Science and Technology, 516, Jungong Road, 200093 Shanghai, China
*Corresponding author: pengji.ding@forbrf.lth.se

Received 29 December 2017; revised 23 January 2018; accepted 9 February 2018; posted 9 February 2018 (Doc. ID 314310); published 1 March 2018

We report on an observation of bi-directional 656 nm lasing action of atomic hydrogen in a premixed CH_4/air flame induced by resonant femtosecond 205 nm two-photon excitation. In particular, the backward-propagating lasing pulse is characterized in the spatial and temporal domains for the sake of a single-ended diagnostic. Its picosecond-scale duration and smooth temporal profile enable spatially resolved detection of hydrogen atoms in the millimeter range, which is successfully demonstrated using two narrow welding flames.

OCIS codes: (120.1740) Combustion diagnostics; (320.2250) Femtosecond phenomena; (190.7110) Ultrafast nonlinear optics; (020.4180) Multiphoton processes.

https://doi.org/10.1364/OL.43.001183

Lasing (or stimulated emission) via resonant optical excitation of species in flame is a widespread phenomenon. Amplified spontaneous emission (ASE) lasing was observed in flame by focusing 5 ns 226 nm laser pulses into an H_2/O_2 flame at sub-atmospheric pressure and room-temperature flows of O_2 and N_2O [1]. Through resonant two-photon excitation, 845 nm lasing of atomic oxygen is generated in both the forward and backward directions. As follows, a lasing effect was also observed in other atoms and molecules such as H [2], C [3], N [4], CO [5], and NH_3 [6]. The backward lasing, propagating in the direction opposite to the pump laser beam, is of particular interest for single-ended combustion diagnostics where only one optical access is available. It should be noted that these earlier works in the field of laser-based combustion diagnostics initiated intensive studies of backward lasing in ambient air during the last decade [7–18], ultimately aiming at remote atmospheric sensing.

The coherent nature of lasing provides some obvious advantages over laser-induced fluorescence detection in signal strength and directionality, suggesting that lasing could be a promising diagnostic technique. In addition, lasing techniques are capable of measuring minor species in combustion processes that other techniques, like Raman scattering or coherent anti-stokes Raman scattering, are unable to detect. However, lasing techniques based on nanosecond pump laser pulses also possess some disadvantages. First, the generation of the lasing pulse along the pump laser beam, as well as its long duration, result in a very poor spatial resolution in the direction of the pump beam, allowing only measurements of vertical profiles [1–3,6]. Secondly, the photochemical production of lasing species distorts the measured signals and, therefore, makes the measurements unreliable [2]. Thirdly, generating lasing emission requires sufficiently high laser power.

In this Letter, we report the generation of backward 656 nm lasing from hydrogen atoms in a flame based on femtosecond two-photon excitation, which is further applied to spatially resolve the hydrogen occurrence in two narrow flames with a resolution of a few millimeters. With the use of a tunable deep-ultraviolet (UV) 125 fs pump laser, a picosecond time-scale 656 nm lasing pulse of atomic hydrogen was generated in a premixed flame in both the forward and backward directions. As shown in Fig. 1(a), the two-photon excitation transition is from the 1S ground state to the 3D excited state using a 205 nm pump laser. It is followed by relaxation from the 3D state to the 2P state (the Balmer-α line), releasing lasing emission at 656 nm wavelength. An increased spectral bandwidth of the pump laser pulse, compared to nanosecond laser pulses, results in a lasing signal with a much broader detuning range of the pump laser wavelength. The characteristics of the backward 656 nm lasing pulse, including emission spectrum, and spatial and temporal profiles, are analyzed. With the backward 656 nm lasing pulses generated from two welding flames, approximately 7 mm spatial resolution for atomic hydrogen detection was achieved, a significant progress towards single-ended diagnostics.

The experimental setup is schematically illustrated in Fig. 1(c). A chirped pulse amplification laser system (Coherent, Hidra-50) is used to deliver 125 fs, 800 nm laser pulses with a maximum energy of 30 mJ at a 10 Hz repetition rate. This laser beam pumps an optical parametric amplifier followed by a frequency mixing apparatus (NirUVis unit), which can provide 205 nm laser pulses with a maximum energy of approximately 40 μJ. The beam diameter is about 5 mm. At first, the 205 nm pump laser beam propagates through a bulk CaF_2 equilateral dispersive prism with an incident angle of

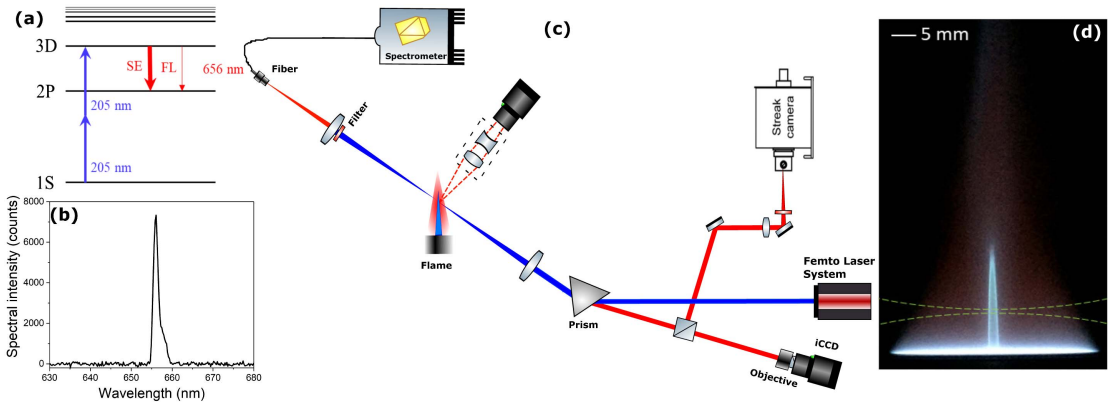

Fig. 1. (a) Energy levels of atomic hydrogen relevant to 205 nm two-photon-excited fluorescence (FL) and stimulated emission (SE). (b) Spectrum of backward 656 nm lasing pulse of atomic hydrogen in a premixed methane/air flame, recorded with a fiber spectrometer (Avantes). (c) Schematic illustration of the experimental setup. (d) Flame-brightness image of the premixed methane/air flame, which clearly shows a much brighter jet flame in the center surrounded by a less bright outer flat flame. The dashed line represents the focusing of the 205 nm femtosecond laser pulses.

31.6°, in order to spatially separate the backward-propagating 656 nm lasing emission from the pump laser beam. In addition, this configuration spectrally purifies the pump laser by dispersing residual frequencies. After the prism, the pulse energy of the pump beam has been reduced to approximate 20 μJ mainly due to reflection losses. Then the pump laser beam is focused by a spherical lens ($f = 300$ mm) into a CH_4/Air flame and creates a two-photon excitation volume of ~100 μm diameter and 2 mm length. A modified porous-plug burner (McKenna) is used [see Fig. 1(d)], which consists of a central tube (2.0 mm inner diameter) and the diameter of the porous plug is 60 mm. Premixed CH_4/Air gas mixtures enter the central tube and the porous plug separately through mass flow controllers. The central jet flame is stabilized on the burner by the surrounding flat flame. The equivalence ratio ϕ was 0.9 for the flat flame and 1.3 for the jet flame.

In the forward direction, a bandpass filter with a central wavelength of 656 nm (Semrock, ~15 nm bandwidth) was used to transmit the induced lasing at 656 nm which was then detected by a calibrated photodiode. In the backward direction, a He–Ne laser operating at a 632.8 nm wavelength was employed to roughly determine the separation angle between the backward 656 nm lasing beam and the 205 nm pump beam outside the dispersive prism. For detection, an intensified charge-coupled device (CCD) camera (Princeton Instrument, PI-MAX 2) was used to capture the spatial profile of the backward 656 nm lasing beam. A streak camera (Optronis OPTOSCOPE) with the capability of 2 ps resolution was used to measure the temporal profile of the lasing pulse. It operated with a streak rate of 10 ps/mm and gain voltage of 880 V; its entrance slit width was set to 0.18 mm.

The emission spectrum of the lasing pulse is presented in Fig. 1(b). By collecting the signal with an $f = 100$ mm lens and putting white papers in front of the detectors, a red spot can be observed by the naked eye in both the forward and backward directions. Unlike the situation with nanosecond/picosecond pumping [1,2,19], where the lasing strength is roughly equal in the two directions, the forward lasing is much brighter than the backward one in our experiments. The stronger forward lasing strength might be due to the traveling wave nature [10,11,15,17], as well as the occurrence of four-wave mixing in the forward direction.

Figure 2 shows the 656 nm lasing excitation spectrum, i.e., the lasing signal versus the pump laser wavelength. The lasing signal was measured with a calibrated photodiode in the forward direction, and each point is the average signal for 500 laser shots. For each point, the central wavelength of the pump laser pulse was also measured before the flame. In order to maintain it while detuning the central wavelength of pump laser pulse, the stability of the pump pulse energy was simultaneously monitored by recording the energy of laser light reflected off the incident surface of the dispersive prism, indicated by the open square symbols in Fig. 2. We can see a broad dependence curve ranging from 204.60 to 205.25 nm, with an optimum pump wavelength of 204.97 nm. The full width at half-maximum (FWHM) of the curve is approximately 0.65 nm (154 cm^{-1}), much broader than the 0.02 nm (~5 cm^{-1}) FWHM observed with nanosecond laser pumping [2]. This is mostly due to the large bandwidth of the 125 fs pump laser

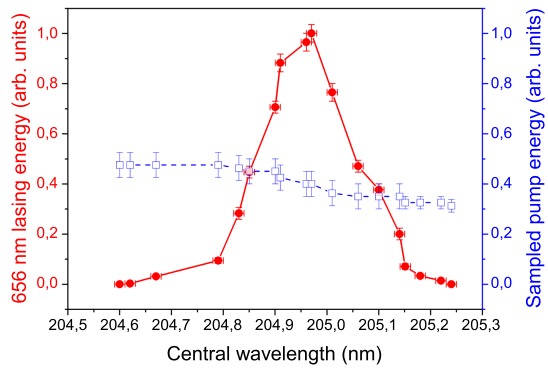

Fig. 2. Pump wavelength scan of femtosecond two-photon-excited 656 nm lasing of atomic hydrogen by using 20 μJ energy pulses in a rich ($\phi = 1.3$) methane/air flame. The open square curve shows the simultaneously sampled pump laser energy.

pulse, resulting in different frequencies with the same spectral phase collectively contributing to the two-photon excitation.

Measuring the pump energy dependence of the lasing intensity provides an excellent mean of establishing the presence of lasing. To control the pulse energy of the pump laser, a variable attenuator was inserted inside the frequency mixing apparatus. The intensity of both the forward and backward 656 nm lasing energies versus pump laser pulse energy is plotted in Fig. 3(a), in which each point corresponds to the average of 10 laser shots. A power function $E_{\text{lasing}} = a + b \times (E_{\text{pump}})^c$ is fitted to the experimental data (dashed curve in the figure) where a, b are coefficients taking into account the presence of the lasing threshold, and c is the power index. It is found that the forward lasing energy scales with a power of 2.1 ± 0.5 power of the pump pulse energy, while the backward lasing energy scales with a power of 2.0 ± 0.2. A threshold energy of approximately 5.5 μJ was determined for both lasing directions. This result is firmly consistent with the expected E^2_{pump} dependence of a two-photon process. For femtosecond two-photon excitation, the interference from photodissociation of other species, such as water, CH_3, and OH, is virtually eliminated [20]. Therefore, only the H atoms that are naturally present in the methane/air flame contribute to the lasing signal, which would facilitate quantification.

Aiming to apply the lasing effect for single-ended combustion diagnostics, we are particularly interested in the backward lasing signal. Figure 3(b) shows a single-shot far-field image recorded with an intensified CCD camera located 1.24 m away from the excitation region in the backward direction. As can be seen, the 656 nm lasing beam has a strong donut-shaped spatial mode, surrounded by a much weaker diffracted mode that was not fully detected due to the limited size of the prism. Considering the excitation region as a pencil-shaped cylindrical emitter, its Fresnel number can be calculated as $F = (\pi w^2)/L\lambda \approx 24$, where $w \approx 100$ μm is the transverse diameter, $L \approx 2.0$ mm is the longitudinal length of the excitation volume, and $\lambda = 656$ nm is the lasing wavelength. Since $F \gg 1$, several diffraction-limited modes can be sustained with the geometrical angle $\theta = w/L = 0.1$, as shown in Fig. 3(b). By neglecting the weak surrounding modes, the divergence of the backward 656 nm lasing beam varies with the pump laser energy such that higher pulse energy results in larger divergence. With a pump pulse energy of 20 μJ, the divergence was determined to ~17 mrad, and the lasing pulse energy was estimated to ~27 pJ using a calibrated photodiode and taking the losses on various optical elements into account.

With a streak camera, the temporal profile of the backward 656 nm lasing pulse is measured as shown in Fig. 3(c). Its duration (FWHM) can be estimated to 20 ps. It is noted that the pulse duration fluctuates around 20 ps because of slight variations of the pump pulse energy. While experiments with nanosecond laser pumping result in lasing pulses of nanosecond duration exhibiting complicated and spiky temporal structures [21,22], our experiments based on femtosecond laser pumping result in lasing pulses of 20 ps duration with smooth temporal profiles, which are very attractive features for spatially resolved single-ended diagnostics.

Considering two spatially separated excitation volumes of hydrogen atoms, these two excitation volumes should give rise to two backward lasing pulses, temporally separated if the lasing pulse durations are sufficiently shorter than the time it takes to travel the distance between the two excitation volumes. To test this idea, two welding torches (1.5 mm nozzle diameter) were used to establish two CH_4/O_2 flames ($\phi = 1.0$) with a separation of 13.5 mm. As shown in Fig. 4, the temporal profile of the backward 656 nm lasing, measured by the streak camera, clearly shows two temporally separated pulses, reflecting the presence of two spatially separated flames. The temporal separation is approximately 55 ps, which corresponds to a spatial separation of 16.5 mm. Given the backward-propagating scheme of lasing pulses introducing a factor of 2, the measured distance between the two flames via a backward lasing technique will be 8.25 mm. We have done the same measurements for different separations of two flames ranging from 7.2 to 19.1 mm. The measured distance versus the actual separation is shown in Fig. 4(c). A linear fit to data leads to a slope of 0.94, suggesting that the backward lasing technique can be a reliable method to spatially resolved measurements. The offset on the "distance" axis could be a result of the combined effect of the nonuniform distribution of the laser intensity along the pump laser path, the slightly different pathways of the two lasing pulses, and the limited temporal resolution of the streak

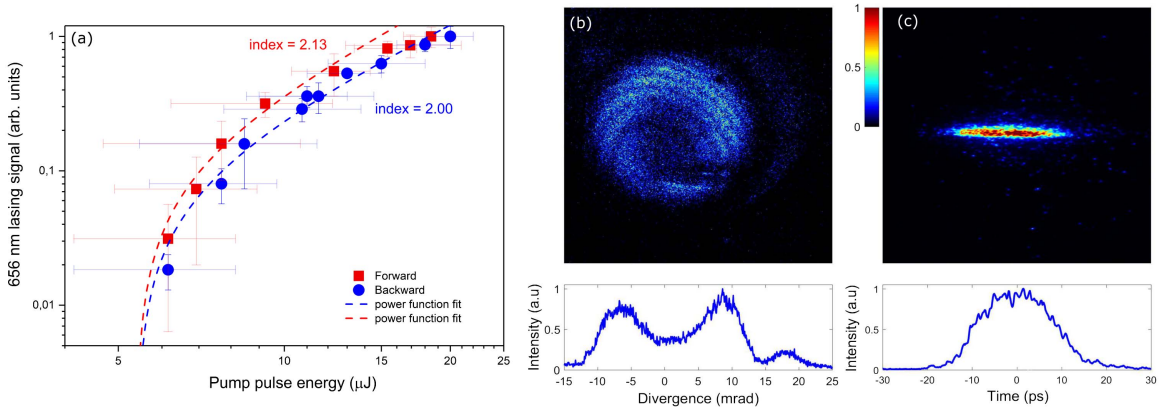

Fig. 3. (a) Pump energy dependences of both forward and backward 656 nm lasing energies. The dashed curves represent power function fitting with a power index of 2.1 and 2.0, respectively. (b) and (c) Single-shot measurement results of the backward 656 nm lasing pulse by using ICCD and streak cameras, respectively. The spatial and temporal profiles are depicted in the lower panels.

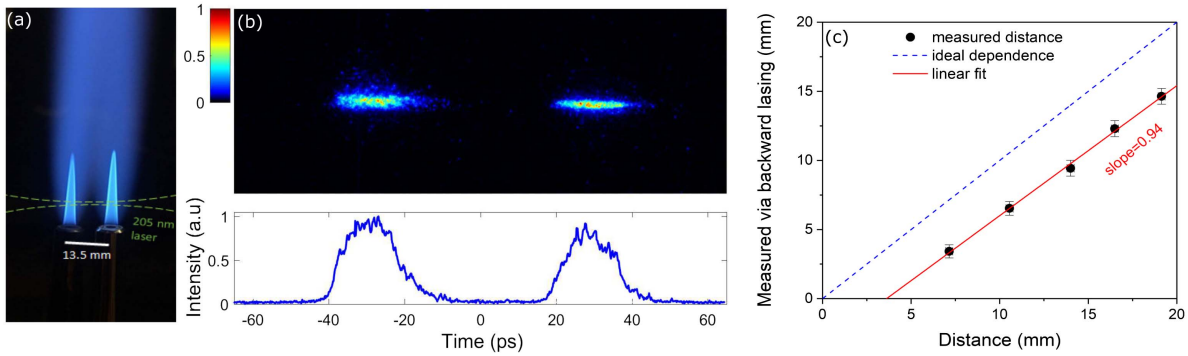

Fig. 4. (a) Image of flames burning on two welding torches, with an illustration of the focusing of the 205 nm laser beam in the center between the two flames. (b) Single-shot temporal profile of the backward 656 nm lasing signal recorded by a streak camera. (c) Measured distance via backward lasing as a function of the actual distance between two flames.

camera. The minimum distance of two flames resolved in our experiments so far was 7.2 mm, limited by the shortest separation of two welding torches. A better spatial resolution of the backward lasing technique can be expected. Due to the fact that 205 nm laser pulses were focused in the midway between two flames, the largest flame separation that can be resolved via a backward lasing technique is limited to around 19 mm. Resolving an arbitrary separation requires a collimated pump laser beam providing high enough pulse energy. Since the lasing effect has been observed in O, N, C, CO, and NH_3 with nanosecond laser pumping, all of which are important species in combustion processes, femtosecond two-photon excited backward lasing of these species, in principle, can be observed under certain experimental conditions. Thus, it appears feasible to extend the present measurement concept towards single-ended spatially resolved detection of these species as well.

In summary, we report on an observation of the backward lasing effect of atomic hydrogen in a premixed methane/air flame using femtosecond deep-UV laser pulses. Following femtosecond resonant two-photon excitation, 656 nm lasing emission occurs in both the forward and backward directions. The characterization of the backward lasing pulse was carried out, including analysis of the emission spectrum, pump energy dependence, and spatial and temporal profiles. The duration of the backward lasing pulse was found to be approximately 20 ps, suggesting a strong potential for spatially resolved measurements of atomic hydrogen in the millimeter range in flames. Using two separated methane/oxygen flames burning on two welding torches, we successfully managed to record two backward 656 nm lasing pulses on a streak camera, with a temporal separation proportional to the spatial separation between the two flames. The minimum separation between two flames that has been resolved was 7.2 mm. Based on these results, we believe that the backward lasing technique holds great potential for single-ended diagnostics, which would constitute a useful tool for combustion diagnostics in intractable geometries with limited optical access.

Funding. Knut och Alice Wallenbergs Stiftelse; TUCLA, H2020 European Research Council (ERC); Swedish Energimyndigheten via the Center for Combustion Science and Technology (CECOST).

Acknowledgment. The authors would like to thank Dr. Andreas Ehn for fruitful discussions of spatially resolved measurements.

REFERENCES

1. M. Aldén, U. Westblom, and J. E. Goldsmith, Opt. Lett. **14**, 305 (1989).
2. J. E. M. Goldsmith, J. Opt. Soc. Am. B **6**, 1979 (1989).
3. M. Aldén, P.-E. Bengtsson, and U. Westblom, Opt. Commun. **71**, 263 (1989).
4. S. Agrup, U. Westblom, and M. Aldén, Chem. Phys. Lett. **170**, 406 (1990).
5. U. Westblom, S. Agrup, M. Aldén, H. M. Hertz, and J. E. Goldsmith, Appl. Phys. B **50**, 487 (1990).
6. N. Georgiev, K. Nyholm, R. Fritzon, and M. Aldén, Opt. Commun. **108**, 71 (1994).
7. Q. Luo, W. Liu, and S. Chin, Appl. Phys. B **76**, 337 (2003).
8. A. Dogariu, J. B. Michael, M. O. Scully, and R. B. Miles, Science **331**, 442 (2011).
9. P. R. Hemmer, R. B. Miles, P. Polynkin, T. Siebert, A. V. Sokolov, P. Sprangle, and M. O. Scully, Proc. Natl. Acad. Sci. USA **108**, 3130 (2011).
10. S. Mitryukovskiy, Y. Liu, P. Ding, A. Houard, and A. Mysyrowicz, Opt. Express **22**, 12750 (2014).
11. P. Ding, S. Mitryukovskiy, A. Houard, E. Oliva, A. Couairon, A. Mysyrowicz, and Y. Liu, Opt. Express **22**, 29964 (2014).
12. Y. Liu, P. Ding, G. Lambert, A. Houard, V. Tikhonchuk, and A. Mysyrowicz, Phys. Rev. Lett. **115**, 133203 (2015).
13. S. Alisauskas, A. Baltuska, R. Boyd, and P. Polynkin, in *European Conference on Lasers and Electro-Optics—European Quantum Electronics Conference* (Optical Society of America, 2015), paper PD_A.
14. T. L. Chng, A. Dogariu, and R. B. Miles, in *47th AIAA Plasmadynamics and Lasers Conference* (American Institute of Aeronautics and Astronautics, 2016), paper AIAA 2016-4142.
15. P. Ding, E. Oliva, A. Houard, A. Mysyrowicz, and Y. Liu, Phys. Rev. A **94**, 043824 (2016).
16. A. Dogariu and R. B. Miles, Opt. Express **24**, A544 (2016).
17. P. Ding, J. C. Escudero, A. Houard, A. Sanchis, J. Vera, S. Vicéns, Y. Liu, and E. Oliva, Phys. Rev. A **96**, 033810 (2017).
18. A. Dogariu and R. Miles, in *Air Lasing*, P. Polynkin and Y. Cheng, eds. (Springer, 2017).
19. A. Laurain, M. Scheller, and P. Polynkin, Phys. Rev. Lett. **113**, 253901 (2014).
20. W. Kulatilaka, J. Gord, V. Katta, and S. Roy, Opt. Lett. **37**, 3051 (2012).
21. R. C. Y. Auyeung, D. G. Cooper, and B. Feldman, Opt. Commun. **79**, 207 (1990).
22. S. Agrup and M. Aldén, Opt. Commun. **113**, 315 (1994).